Eur. Phys. J. B **59**, 259–269 (2007)
DOI: 10.1140/epjb/e2007-00285-1

THE EUROPEAN PHYSICAL JOURNAL B

Noise-controlled slow–fast oscillations in predator–prey models with the Beddington functional response

R. Mankin, T. Laas[a], E. Soika, and A. Ainsaar

Department of Natural Sciences, Tallinn University, 25 Narva Road, 10120 Tallinn, Estonia

Received 19 June 2007 / Received in final form 31 August 2007
Published online 17 October 2007 – © EDP Sciences, Società Italiana di Fisica, Springer-Verlag 2007

Abstract. The influence of environmental fluctuations (modeled as a multiplicative dichotomous noise) on predator–prey interaction is studied using a metapopulation model with N prey-subpopulations. Investigating the role that predator interference plays in the dynamics of such trophic systems, the Beddington functional response is considered. In case the growth rates of prey and predator are widely different, we obtain analytic results by a dynamical mean-field approximation. In some regions of the system parameters, variations of noise amplitude or correlation time can cause transitions of the mean field from a globally stable equilibrium to the stable limit cycle as well as in the opposite direction. The conditions for the occurrence of such a phenomenon are found and illustrated by phase diagrams. Implications of the results on the colored-noise-induced extinction of a predator population are also discussed.

PACS. 05.40.-a Fluctuation phenomena, random processes, noise, and Brownian motion – 87.10.+e General theory and mathematical aspects – 87.23.Cc Population dynamics and ecological pattern formation

1 Introduction

Within the past two decades noise-dependent behavior of nonlinear systems has received considerable attention. Some recent discoveries have inspired the idea that noise can induce order in nonlinear nonequilibrium systems. Stochastic resonance [1], noise-induced phase transitions in spatially extended systems [2], stochastic transport in ratchets [3], noise-induced spatial patterns [2], coherence resonance [4], hypersensitive response [5], noise-induced multistability and discontinuous transitions [6,7] are a few new phenomena in this field. Active analytical and numerical studies of various relevant models have been stimulated by their possible applications in chemical physics, molecular biology, nanotechnology, and separation techniques of nanoobjects [3,8,9]. Recently, the essential role of environmental fluctuations has been recognized in theoretical ecology. Noise-induced effects on population dynamics have been subject to intense theoretical investigations [10]. Those include, for example, noise-induced oscillations in two competing species [11], stochastic resonance in population dynamics [12], extinction statistics in N random interacting species [13], and transient dynamics of ecosystems in the presence of colored noise [14].

The problem how environmental fluctuations and species interaction may determine oscillations in population sizes, displayed by many organisms in nature as well as in laboratory cultures [15–17], is one of the central issues in ecology. The most widely accepted deterministic (without fluctuations) model for predator–prey dynamics can be written as follows [16,18]:

$$\begin{aligned} \frac{dx}{dt} &= xf(x) - \alpha g(x,y)y, \\ \frac{dy}{dt} &= y[\beta g(x,y) - d], \end{aligned} \tag{1}$$

where x and y are densities of prey abundance and predator abundance, respectively, $f(x)$ is the per capita rate of increase of the prey in absence of predation, and d is food-independent predator mortality, assumed to be constant. The function αg describes the amount of prey consumed per predator per unit time, while βg describes predator production per capita. The quotient of the two constants β and α is the conversion efficiency β/α. During the past decade a lot of studies have been devoted to the consequences of assuming either a prey-dependent, $g = g(x)$, or ratio-dependent, $g = g(x/y)$, predator functional response (a trophic function) in predator–prey models [18–20]. Ratio-dependent models can display original dynamic properties that have never been observed in the most popular prey-dependent models. For example, the origin ($x = 0, y = 0$) can be a node simultaneously attractive and repulsive, thus shedding a new light on ecological extinction. A coexistence of several dynamic regimes with the same set of parameters can also be observed [21]. These are realistic features since those

[a] e-mail: tony@tlu.ee

behaviors have been observed experimentally [22]. However, it has been recognized that pure prey dependence or ratio dependence are both likely to be rare in nature [23]. Namely, the specific prey-dependent form $g(x)$ is the extreme case of "non-sharing" predation process in case individuals are uniformly distributed in space and their age structure and sex ratio do not significantly affect the growth rate of either population; the ratio-dependent form $g(x/y)$ is the extreme case of "perfect sharing" and corresponds to the case of heterogeneous systems, where the large-scale outcome of predation is a sharing process (the predators have to search or compete for food) [18]. In the present paper we use the word "interference" to designate any mechanism by which predator density depresses individual predator performance. In this context, ratio-dependence can be considered as an extreme case of strong mutual interference between predators [24]. Using a mechanistic approach to describe predator behavior, Beddington [25] developed an explicit model to describe the effect of predator interference on the trophic function:

$$g(x,y) = \frac{x}{x + by + c}, \tag{2}$$

where b is a predator interference parameter, and c is a saturation constant. It is remarkable that, independently, DeAngelis et al. [26] have developed the same model followed by a phenomenological approach on the scale of populations. Actually, equation (2) can be regarded as a quite general trophic function [20,24]. First, equation (2) has been derived from general mechanistic assumptions (see also [25,27]). Second, most popular functional responses, such as the Holling type II prey-dependent functional response ($b = 0$ in Eq. (2)) [20,24] and the Michaelis-Menten-Holling type ratio-dependent functional response ($c = 0$ in Eq. (2)) [18,20], are particular cases of equation (2).

Although deterministic predator–prey models with the Beddington functional response (BFR) are useful in modeling many real ecological communities and have been subject to intense theoretical investigations (particularly the ratio-dependent limit) [20,21,24,28], there is hardly anything available either on qualitative analysis of multispecies interaction or on the effect of environmental fluctuations in models based on the BFR or on a ratio-dependent approach [29,30].

Recently we have considered a broad class of $(N+1)$-species ratio-dependent predator–prey models that consist of one predator population and N prey populations with fluctuating carrying capacities [29]. Notably, in the framework of the mean field theory it is shown that the dynamical system for the mean prey abundance and predator abundance exhibits Hopf bifurcations with respect to the noise correlation time.

However, this work is based on local stability analysis with the assumption that noise dispersion (or amplitude) is very small. As a consequence, for the existence of the phenomenon of noise-induced Hopf bifurcations the control parameter (prey capturing rate α) must be located very near the bifurcation point α_{cr} of the corresponding deterministic model. Moreover, in the case considered in [29] the trivial equilibrium ($x = 0, y = 0$) has its own basin of attraction, even if there exists a nontrivial stable or unstable (with a stable limit cycle) equilibrium. Hence, the appearance of noise-induced Hopf bifurcation is very sensitive to small variations of the system parameters and initial conditions, and so, the results of [29] are mainly of a theoretical interest, while biological applications in nature seem impossible. Thus, [29] leaves open the fundamental question in the ecological context, both from the theoretical and practical viewpoints, whether environmental colored fluctuations with a finite amplitude can cause globally asymptotically stable limit cycles in ratio-dependent (or in the case of the BFR) predator–prey systems, i.e. whether transitions from equilibrium states to oscillatory regimes (and the opposite way) sometimes occurring in ecosystems [15–17] could be regarded as induced by environmental nonequilibrium fluctuations. The question is addressed in the present paper and the answer is affirmative, which is a crucial result, allowing in practice to link the transitions between an oscillatory regime and an equilibrium state of population sizes observed in nature with changes of environmental fluctuations.

So in the present paper we considerably generalize the model used in [29], enlarging the dimension of the system parameter space by two. Namely, in our calculations we allow the noise amplitude to take any biologically reasonable values (including moderate ones) and replace the ratio-dependent functional response by the Beddington trophic function (the ratio-dependent model is a particular limit case). Making the model more general and intricate enables us to understand the interrelationship of some effects which formerly seemed to stand apart, and thereby reveal some new features. Thus, we consider a class of $(N+1)$-species predator–prey models with the BFR that consist of one predator population and N prey populations. The effect of a fluctuating environment on the prey populations is modeled as colored fluctuations of the carrying capacities. For the sake of mathematical simplicity, we confine ourselves to the case where the noise is a dichotomous Markovian noise, also known as the random telegraph signal [31]. Since one of the characteristic quantities of an ecosystem, perhaps the most fundamental one, is its average species density [32] ($\sum_{i=1}^{N} X_i/N$, where X_i is the population density of the ith species), we consider the average species density of prey as one of the two state parameters of an ecosystem (or a metapopulation), the other state parameter being the density of predator abundance. We study the model using the mean field approach, focusing on colored-noise-induced transitions. Differing from [29] we consider here that region of the system parameters space where the corresponding deterministic model is characterized by a nontrivial globally asymptotically stable equilibrium.

The main contribution of this paper is as follows.

In predator–prey systems in which the growth rate of the predator is much smaller than the growth rates of preys, we establish colored-noise-induced transitions from a globally stable equilibrium to the stable limit cycle (with some oscillations of population abundances) as well as

in the opposite direction. Furthermore, the transition is found to be reentrant, e.g., if the noise amplitude is greater than a certain threshold value, then the limit cycle appears above a critical value of the noise correlation time, but disappears again through reentrant transition to the equilibrium state at a higher value of the noise correlation time. In the case of logistic self-regulation of prey we give the necessary and sufficient conditions for the appearance of such effects. We emphasize that contrary to the particular case of a ratio-dependent model described in [29], here the limit cycles rather occur at moderate or greater noise amplitudes than at very small ones. We also analyze the role of the predator interference parameter and saturation constant of the BFR in such transitions. Moreover, in the cases of moderate and small predator interference we establish colored-noise-induced transitions from a steady state to the state where the predator population extincts, and also derive the conditions for the existence of such, very important in an ecological viewpoint, phenomenon (in the case of a ratio-dependent model such transitions are absent).

The structure of the paper is as follows. In Section 2 we present a brief review of the properties of a deterministic model (1) with the BFR. The basic model investigated in this work is presented. A mean-field description of the model is given and the corresponding self-consistency equations are found. Section 3 analyzes the behavior of the self-consistently determined mean field. The phenomena of colored-noise-induced relaxation oscillations of prey and predator densities and colored-noise-induced extinction of the predator population are established, and the conditions for such effects are illustrated with the help of phase diagrams in the system parameters space. Section 4 contains some brief concluding remarks.

2 Model

2.1 A deterministic predator–prey system with the Beddington functional response

Recently, a complete mathematical description of the deterministic predator-prey systems (1) with Beddington functional response (2) and with the logistic self-regulation

$$f(x) = \delta\left(1 - \frac{x}{K}\right), \tag{3}$$

where K is the carrying capacity of the prey and δ is a constant intrinsic growth rate, have been the topic of a number of investigations [24,28]. The main objective of those papers is to consider the stability behavior of solutions around different equilibrium points (x_e, y_e). The biological role played by predator interference in the stabilization of such systems is investigated in [24]. If the initial conditions lie within the positive quadrant ($x(0) = x_0 > 0, y(0) = y_0 > 0$), then it is known [28] that the solutions of system (1) with equations (2) and (3) are positive and bounded for all $t \geq 0$. The predator–prey system described above has two equilibria, $E_1 = (0,0)$ and $E_2 = (K,0)$, for all biologically possible values of the parameters ($\alpha > 0, \beta > 0, d > 0, \delta > 0, K > 0, b > 0$, and $c > 0$). The third equilibrium point $E_3 = (x_s, y_s)$, i.e., the nontrivial equilibrium is given by

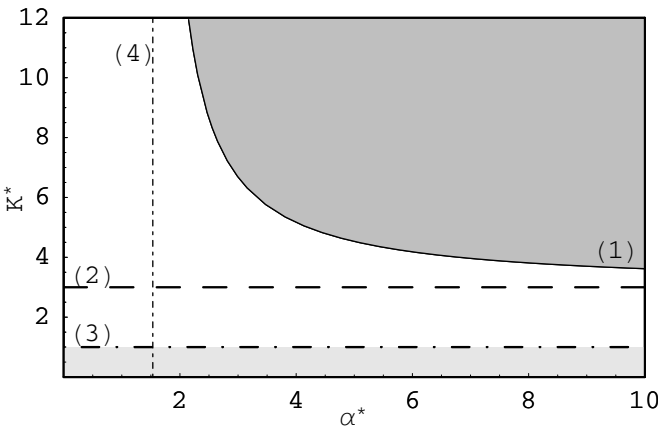

Fig. 1. Existence and stability of equilibriums and limit cycles in relation to ratios $\alpha/b = \alpha^*$ and $K/c = K^*$ (the deterministic model (1)–(3) with parameter values $s = 0.5$; $\delta = 1.0$; $d = 0.3$). The stability region of a nontrivial equilibrium E_3 is shown in white, the existence of a stable trivial equilibrium $E_2 = (0, K)$ in light grey (E_3 is absent), and the existence of stable limit cycles in dark grey. Solid line (1): the Hopf bifurcation curve (see Eq. (8)). Dashed line (2) is the asymptotic limit $K/c = (1+s)/(1-s) = 3$ of curve (1). Dashed-dotted line (3): $K/c = s/(1-s) = 1$. Dotted line (4) depicts the lower limit on α/b for the existence of Hopf bifurcations (see Eq. (9)).

$$x_s = \frac{K}{2}\left[1 - \frac{\alpha(1-s)}{\delta b} + \sqrt{\frac{4\alpha s c}{\delta b K} + \left(1 - \frac{\alpha(1-s)}{\delta b}\right)^2}\ \right],$$
$$y_s = \frac{1}{sb}[x_s(1-s) - cs], \qquad s := \frac{d}{\beta}. \tag{4}$$

This equilibrium is biologically meaningful ($x_s > 0, y_s > 0$) only if

$$\frac{K}{c} > \frac{s}{1-s}, \qquad 0 < s < 1, \tag{5}$$

i.e., the predators and prey coexist in equilibrium provided the maximal predator growth rate β is larger than its death rate d and the saturation parameter c is sufficiently small. The stability analysis of E_i shows that the equilibrium $E_1(0,0)$ is always unstable (a saddle point) and the equilibrium $E_2 = (K,0)$ is a saddle point (unstable) if the conditions (5) are fulfilled, while in the opposite case E_2 is globally asymptotically stable. In the latter case predators go to extinction. The behavior of the nontrivial equilibrium $E_3 = (x_s, y_s)$ is more complicated [28].

In the rest of the paper, we shall always assume that the maximal predator growth rate β is restricted to the inequalities

$$d < \beta < \delta + d. \tag{6}$$

In this case the existence and stability of a positive nontrivial equilibrium in relation to the carrying capacity K and prey capturing rate α are illustrated in Figure 1.

There is a lower limit on K/c for the existence of a non-trivial equilibrium E_3:

$$\left(\frac{K}{c}\right)_1 = \frac{s}{1-s}. \tag{7}$$

For $s/(1-s) < K/c < (1+s)/(1-s)$, we always have the global asymptotic stability of E_3. For a greater K/c, $(K/c) > (1+s)/(1-s)$, there is an upper limit on α/b for the stability of E_3. One can find the critical curve $(K/c)_{cr}$:

$$\left(\frac{K}{c}\right)_{cr} = \frac{\left[\frac{\alpha}{b}(1+s)-d\right]^2}{(1-s^2)\left(\frac{\alpha}{b}-\beta\right)\left[\frac{\alpha}{b}-\left(\frac{\alpha}{b}\right)_{cr}\right]}, \tag{8}$$

$$\left(\frac{\alpha}{b}\right)_{cr} = \frac{\delta + d(1-s)}{1-s^2}, \tag{9}$$

above which the equilibrium E_3 is unstable and there exists exactly one limit cycle which is globally asymptotically stable [28], i.e., the predator and prey populations oscillate periodically. Under assumption (6), it is clear from equations (8) and (9) that there will be a limit cycle at some values of s and d if and only if

$$\frac{\alpha}{b} > \delta, \qquad \frac{K}{c} > \frac{\alpha}{\alpha - b\delta}. \tag{10}$$

Finally, we emphasize that the dynamical behavior of the deterministic predator–prey model (1) with the BFR and logistic self-regulation depends only on the ratios K/c and α/b, but not on all four parameters (α, K, c, b) independently.

2.2 Stochastic model

As was mentioned in Introduction, the present model is based on a generalization of the predator-prey dynamics (1) with the BFR (see Eq. (2)) and with logistic self-regulation (3) to the case of one predator population and N prey populations (see also [29]):

$$\frac{dX_i}{d\tilde{t}} = X_i f_i(X_i) - \tilde{\alpha} g(\bar{x}, y)\frac{y}{\bar{x}} X_i,$$
$$\frac{dy}{d\tilde{t}} = \tilde{\beta} y g(\bar{x}, y) - \tilde{d} y, \tag{11}$$

where $X_i(\tilde{t})$ $(i = 1, \ldots, N)$ is the density of the ith prey population at the time $\tilde{t}$, $y(\tilde{t})$ is the density of the predator population, and $\bar{x}(\tilde{t}) = (1/N)\sum_{i=1}^{N} X_i(\tilde{t})$ is the average of the prey population densities. The positive constants $\tilde{\alpha}$, $\tilde{\beta}$, and $\tilde{d}$ stand for the prey capturing rate, maximal predator growth rate, and predator death rate, respectively. Here we have assumed that for consumers (predator) all prey populations are equivalent, so that the function $\tilde{\alpha} g(\bar{x}, y) X_i/\bar{x}$ describes the amount of the ith prey consumed per predator per unit time. The following analysis applies to the Beddington functional response $g(\bar{x}, y)$ where x is replaced by $\bar{x}$ (see Eq. (2)). A typical mechanism for self-regulation in ecosystems includes, for example, territorial breeding requirements and the crowding effect caused by competition for resources [32]. These are taken into account by applying the logistic self-regulation model (3)

$$f_i(X_i) = \delta\left(1 - \frac{X_i}{K_i}\right), \tag{12}$$

where K_i is the carrying capacity of the ith species.

Random interaction with the environment (climate, diseases, etc.) is taken into account by introducing a colored noise in $f_i(X_i)$. From now on we shall use fluctuations of the carrying capacity

$$K_i = K[1 + aZ_i(\tilde{t})], \tag{13}$$

where colored noise $Z_i(\tilde{t})$ is assumed to be a dichotomous Markovian stochastic process [31]. A dichotomous process is a random stationary Markovian process consisting of jumps between two values $z = -1, 1$. The jumps follow in time according to a Poisson process, while the values occur with the stationary probability $1/2$. The mean values of $Z_i(\tilde{t})$ and the correlation function are

$$\langle Z_i(\tilde{t})\rangle = 0, \quad \langle Z_i(\tilde{t}) Z_j(\tilde{t}')\rangle = \delta_{ij}\exp(-\tilde{\nu}|\tilde{t} - \tilde{t}'|), \tag{14}$$

where δ_{ij} is the Kronecker symbol and the switching rate $\tilde{\nu}$ is the reciprocal of the noise correlation time $\tilde{\nu} = 1/\tilde{\tau}_c$. Obviously, model (11) with equations (12) and (13) is biologically meaningful only if

$$a < 1. \tag{15}$$

It is practicable, by applying the properties of the dichotomous process, to convert the term K_i^{-1} in equation (12) to the form

$$K_i^{-1} = \gamma[1 - aZ_i(\tilde{t})], \quad \gamma = \frac{1}{K(1-a^2)}. \tag{16}$$

By substituting identity (16) into equations (12) and (11) and applying a scaling of the form

$$t = \delta\tilde{t}, \quad \nu = \frac{\tilde{\nu}}{\delta}, \quad \alpha = \frac{\tilde{\alpha}}{\delta}, \quad \beta = \frac{\tilde{\beta}}{\delta}, \quad d = \frac{\tilde{d}}{\delta} \tag{17}$$

we get a dimensionless formulation of the dynamics

$$\frac{dX_i(t)}{dt} = X_i(t)\left\{1 - \gamma[1 - aZ_i(t)]X_i(t) - \alpha g(\bar{x}, y)\frac{y}{\bar{x}}\right\},$$
$$\frac{dy(t)}{dt} = y(t)[\beta g(\bar{x}, y) - d], \qquad i = 1, \ldots, N, \tag{18}$$

where $Z_i(t)$ is a dichotomous noise with the amplitude 1 and a switching rate ν. We emphasize that equations (18) are mathematically equivalent to the initial system (11), (12) and (13) and have been derived without any approximation. Note that if noise is absent and the distribution of the initial prey population abundances is uniform, $x_i(0) = x_0$, then the model (18) reduces to the deterministic predator–prey model (1) with equations (2) and (3) for $\bar{x}$ and y, i.e.

$$\frac{d\bar{x}}{dt} = \bar{x}\left[1 - \gamma\bar{x} - \alpha g(\bar{x}, y)\frac{y}{\bar{x}}\right],$$
$$\frac{dy}{dt} = y\beta[g(\bar{x}, y) - s], \qquad s = \frac{d}{\beta}. \tag{19}$$

Thus, in this case, the results described in [24,28] are immediately applicable (see also Sect. 2.1).

2.3 Mean field approximation

To proceed with the analytical examination of Model (18), we follow the mean field approximation scheme. We assume that $N \to \infty$. This means that we are interested in the case of a very great number of prey populations (or subpopulations in a prey metapopulation). The mean field approximation can be reached by replacing the size average $\bar{x} = (1/N)\sum_{i=1}^{N} X_i(t)$ by the statistical average $\langle X(t)\rangle$ in equations (18). Hence, each stochastic differential equation for $X_i(t)$ in equations (18) can be reduced to a stochastic differential equation with a dichotomous noise of the form

$$\frac{dX(t)}{dt} = X(t)\{\rho(t) - \gamma X(t)[1 - aZ(t)]\}, \qquad (20)$$

where

$$\rho(t) = 1 - \alpha g\big(\langle X(t)\rangle, y(t)\big)\frac{y(t)}{\langle X(t)\rangle}. \qquad (21)$$

According to [31], the corresponding composite master equation is

$$\frac{\partial}{\partial t}P_n(x,t) = -\frac{\partial}{\partial x}\{x[\rho - \gamma x(1-a_n)]P_n(x,t)\} - \frac{\nu}{2}\sum_{m=1}^{2}[(2\delta_{nm}-1)P_m(x,t)], \qquad (22)$$

with $P_n(x,t)$ denoting the probability density for the combined process (x, a_n, t); $n, m = 1, 2$; $-a_1 = a_2 = a$.

If the predator population density y is constant (or a very slow variable) and $\rho > 0$, then significant inequalities follow from equation (20) to characterize the stationary state (or the quasistationary state) of the system. For a stationary case, $x_1 = \rho/[\gamma(1-a)]$ and $x_2 = \rho/[\gamma(1+a)]$ are stable fixed points of the deterministic equations (20) with $Z(t) = 1$ and $Z(t) = -1$, respectively, and all trajectories $X(t)$ satisfy the following inequalities:

$$\frac{\rho}{\gamma(1-a)} > X(t) > \frac{\rho}{\gamma(1+a)}. \qquad (23)$$

Now, the behavior of the stationary system (20) can be analytically studied by means of a standard mean field theory procedure [2]. For a stationary state we can solve equation (22), taking as the boundary condition that there is no probability current at the boundary (23). This way we get the stationary probability distribution in the x space, $P(x,\rho) = \sum_n P_n^s(x)$, where $P_n^s(x)$ is the stationary probability density for the state (x, a_n). After quite simple calculations one can find (cf. [33])

$$P(x,\rho) = \frac{\rho}{\gamma a B\big(1/2, \nu/(2\rho)\big)x^2} \times \left|1 - \frac{\rho^2}{\gamma^2 a^2}\left(\frac{\gamma}{\rho} - \frac{1}{x}\right)^2\right|^{[\nu/(2\rho)]-1}, \qquad (24)$$

where $\rho = 1 - \alpha g(\langle X\rangle, y)y/\langle X\rangle$, $B(\lambda,\kappa) = \Gamma(\lambda)\Gamma(\kappa)/\Gamma(\lambda+\kappa)$ is the beta function, and Γ is the gamma function. The probability density $P(x,\rho)$ is normalized to restrict x within the interval (x_1, x_2). The self-consistency equation for the Weiss mean field approach, whose solution yields the dependence of $\langle X\rangle$ on the system parameters, is

$$\langle X\rangle = \int_{x_2}^{x_1} xP(x,\rho)dx. \qquad (25)$$

With the help of the stationary probability distribution (24), one can easily calculate the moments of prey population densities

$$\langle X^k\rangle = \left(\frac{\rho}{\gamma}\right)^k {}_2F_1\left(\frac{k}{2}, \frac{k}{2}+\frac{1}{2}; \frac{\nu}{2\rho}+\frac{1}{2}; a^2\right), \qquad (26)$$

where ${}_2F_1$ is the hypergeometric function and $k = 1, 2, \ldots$

3 Relaxation oscillations

3.1 Isoclines

In this section, we discuss a special case where $\tilde{\beta} \ll \delta$ ($\beta \ll 1$; relaxation oscillation limit), i.e., the case where the maximal predator growth rate is much less than the maximal prey growth rate. Interaction of fast and slow processes is an integral part of the sudden large shifts that sometimes occur in ecosystems [34]. There is a range of examples from natural as well as exploited aquatic and terrestrial systems, where catastrophic bifurcations in the dynamics of the fast components are at the heart of such dramatic shifts [34,35]. Famous examples are the spruce-budworm interaction [36] (the dynamics of the budworm is much faster than that of the spruce trees on which they forage) and plankton pelagic communities (preys, fast variable) and fish populations (predators, slow variable) [34].

It is shown by the last equation of equations (18) that in the limit $\beta \ll 1$, y varies very slowly. Since the dynamics of X (see Eq. (20)) is much faster than that of y, a quasi-stationary probability distribution is formed before y varies. In other words, the variable y in equation (20) is just a parameter for the dynamics of X. In this case, we can investigate the mean field dynamics of the system (18) using the following equations (see also Eq. (26)):

$$y = \frac{c(1-\rho)}{b(\alpha^* + \rho - 1)}[F(\rho) + 1], \quad \alpha^* \equiv \frac{\alpha}{b}, \qquad (27)$$

$$\frac{dy}{dt} = \beta y\left[\frac{u(\rho)}{1+u(\rho)} - s\right],$$

$$\rho \in \begin{cases} (1-\alpha^*, 1) & \text{if } \alpha^* \le 1, \\ (0,1) & \text{if } \alpha^* \ge 1, \end{cases} \qquad (28)$$

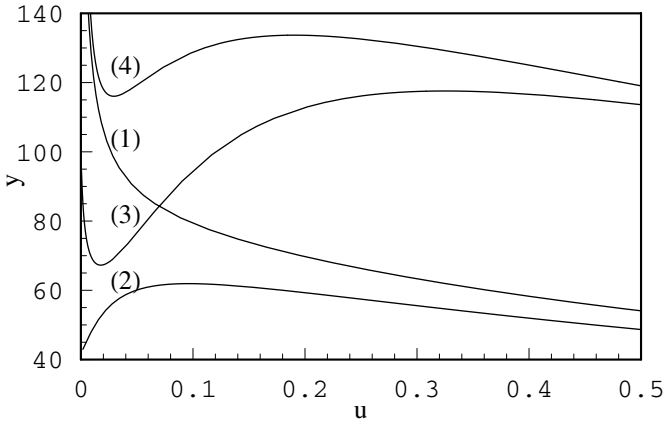

Fig. 2. The prey isoclines $y(u)$ vs the parameter u. Curves (1)–(4) correspond to the following parameters: (1) $a = 0$, $\alpha^* = \alpha/b = 1.002$, $K^* = K/c = 80$; (2) $a = 0$, $\alpha^* = 1.024$, $K^* = 75$; (3) $a^2 = 0.82$, $\nu = 0.08$, $\alpha^* = 1.01$, $K^* = 230$; (4) $a^2 = 0.9$, $\nu = 0.04$, $\alpha^* = 0.9$, $K^* = 210$. The isoclines have been computed by means of equations (27) and (29) at $c/b = 1.0$.

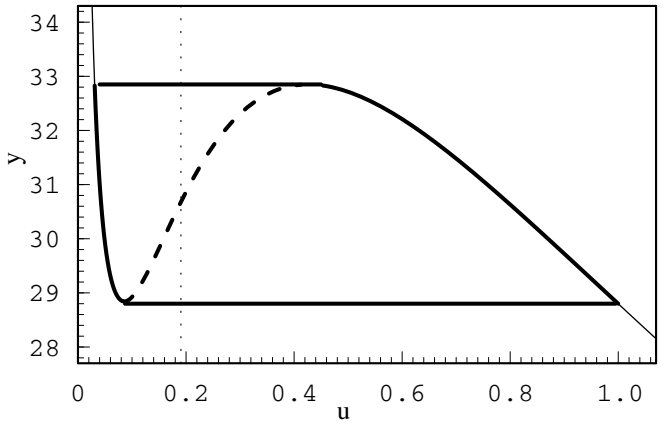

Fig. 3. Noise-induced relaxation oscillations. The thick solid cycle depicts the predator population density y versus the ratio $u = \langle X\rangle/(by + c)$, computed by means of equations (27), (29), (30), and (31). Solid lines: the stable pieces of the prey isocline determined by equations (27) and (29). Dashed line: the unstable piece of the prey isocline. Dotted line: the predator isocline given by equation (31). Parameter values: $c/b = 1.0$, $\alpha^* = 0.99$, $K^* = 100$, $a^2 = 0.9$, $\nu = 0.2$, and $s = 0.16$. The oscillation cycle follows a stable piece of the prey isocline and jumps to another stable branch of the isocline.

where for convenience we have used the notations

$$u(\rho) = \frac{\langle X\rangle}{by + c} = \frac{(\alpha^* + \rho - 1)F(\rho)}{(1-\rho)F(\rho) + \alpha^*}, \tag{29}$$

$$F(\rho) = K^*(1-a^2)\rho\ {}_2F_1\left(\frac{1}{2}, 1; \frac{1}{2} + \frac{\nu}{2\rho}; a^2\right), \quad K^* = \frac{K}{c}. \tag{30}$$

Note that $u(\rho)$ is a monotonically increasing function on ρ and the upper value of ρ, $\rho = 1$, corresponds to the extinction of the predator population. Equations (27) and (29) correspond to the prey isocline of the system. It is obvious that the predator isocline is given by

$$u = \frac{s}{1-s} = \text{const.} \tag{31}$$

The slow–fast approach suggests an intuitive idea why predator–prey cycles sometimes occur. This can happen if the fast system (20) can have fold bifurcations of the mean field in the range of interest of the parameter y, i.e., if the self-consistency equations (27) and (29) can have more than one solution $u(y)$ in some interval of the values of y. The typical forms of the prey isocline $y(u)$ are represented in Figure 2. At the condition (6), one has to discern four cases.

For $\alpha^* < 1$ and in the case of $\alpha^* > 1$, $K^* < \alpha^*/(\alpha^* - 1)$ the deterministic counterpart ($a = 0$) of the curve $y(u)$ is described with a monotonically decreasing function as the variable u increases (see curve (1) in Fig. 2). Obviously the system is monostable and no cycle can occur. In the deterministic case, if the conditions (10), i.e. $\alpha^* > 1$, $K^* > \alpha^*/(\alpha^* - 1)$, are valid, there occurs a nonmonotonic dependence with one extremum of the prey isocline $y(u)$ on u (curve (2) in Fig. 2). In this case the cycles are possible and occur when the predator isocline $u = s/(1-s)$ intersects the unstable piece of the prey isocline, i.e. when it intersects the increasing branch of the prey isocline. The presence of colored fluctuations of the carrying capacities of preys has a qualitative influence on the forms of the isocline $y(u)$, so that in some regions of the noise parameters a and ν the prey isocline $y(u)$ can have two extrema. The corresponding isoclines are represented in Figure 2 with curves (3) and (4). Contrary to curve (3), on curve (4) the value of $y(0)$ is greater than the value of y at the local maximum. Although cycles are possible in both cases, pure relaxation oscillations can appear only for prey isoclines of the form (4). In this case the relaxation cycles occur when the predator isocline $u = s/(1-s)$ intersects the unstable (increasing) branch of $y(u)$ (see Fig. 3). Thus, in the last mentioned case, the system will converge to a limit cycle, represented in Figure 3, starting from any initial state $y(0) > 0$ and $\langle X(0)\rangle > 0$. A long time series of abundances of predators and prey (Fig. 4) illustrates the fact that cycles are characterized by periods of relatively little change, separated by dramatic transitions in the ecosystem. That is why in ecological context such cycles are also called slow–fast cycles [34]. It is seen that the amplitudes of population size oscillations are relatively large. In addition the phase lag (the delay between prey and predator maxima) as a fraction of the cycle period $T = 161.61$ is 0.31, which is greater than in the case of "classical" predator–prey cycles (the quarter-cycle delay). As mentioned above the oscillatory regime of predator–prey communities can also appear if the prey isoclines behave as curves (2) and (3) in Figure 2. But in these cases the slow-fast approach considered is invalid at low values of prey densities X where the dynamics of X (see Eq. (20)) is slower than that of the predator density y. Moreover, in last cases, under the condition $\tilde{\beta} \ll \delta$ the dynamics can

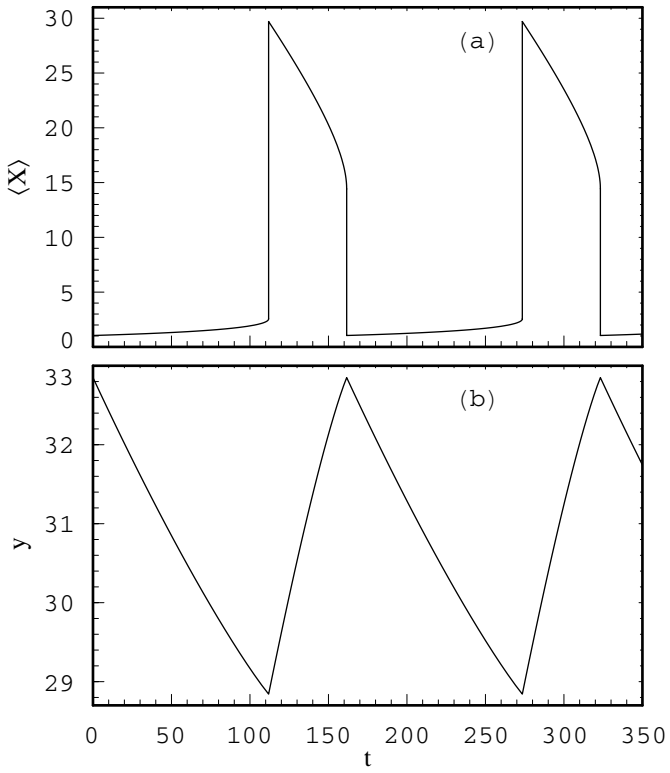

Fig. 4. Time evolution of the mean prey density $\langle X\rangle$ (panel (a)) and predator density y (panel (b)) obtained by numerically solving equations (27)–(30) for the limit cycle displayed in Figure 3 at $\beta = 0.01$. Note that the predator–prey cycles exhibit a delay of $\Delta t \approx 49.73$ between the prey and predator maxima. Time is dimensionless as scaled by equation (17).

come very close to the axes ($x = 0, y = 0$), and extinction may occur in nature due to demographic or environmental stochasticity. Therefore, in ecological context the problem of the existence of noise-induced slow-fast cycles is reduced to finding such regions of noise parameters where prey isoclines of the form (4) (see Fig. 2) are possible.

3.2 Noise-induced transitions

First, we examine the case in which the predator interference parameter b is larger than the prey capturing rate α, i.e. $\alpha^* < 1$. This case is important to study, because it permits to identify the cases in which the relaxation oscillations are solely due to colored noise. Here we would like to remind the reader of the fact that the corresponding deterministic model (19) with conditions $K/c > s/(1-s)$ has a globally asymptotically stable nontrivial equilibrium; the corresponding prey isocline $y(u)$ is a monotonically decreasing function of u. At $\alpha^* < 1$ two cases can be discerned. (i) If the carrying capacity K^* is less than a critical value K_c^*, the prey isocline $y(u)$ is always described with a monotonically decreasing function of u and the system is monostable, i.e., no limit cycle can occur. The critical

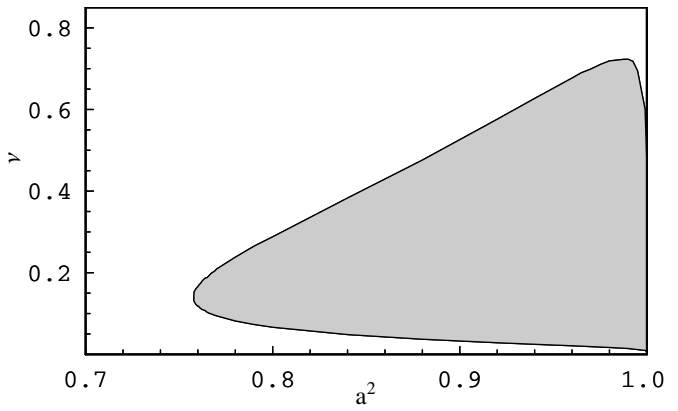

Fig. 5. A plot of the phase diagram in the $\nu - a^2$ plane at $\alpha^* = 0.99$ and $K^* = 100$. The shaded domain corresponds to the region where noise-induced relaxation oscillations are possible. The borders of the shaded region are computed from equations (34), (27), (29), and (30). Note that at $a^2 = 1$ both borders approach zero.

carrying capacity K_c^* is given by the equations

$$K_c^* = \frac{2z^*(1+z^*)e^{z^*}}{2(1-\alpha^*)+z^*(2-\alpha^*)}, \tag{32}$$

where z^* is the positive root of the algebraic equation

$$z^3 + \frac{4(\alpha^*-1)}{\alpha^*}z^2 - 2\left[1 - \frac{4(\alpha^*-1)}{\alpha^*}\right]z + \frac{4(\alpha^*-1)}{\alpha^*} = 0. \tag{33}$$

Note, that the formula (32) for K_c^* can be easily find from equations (27) and (29) at the upper limit of the noise amplitude, $a \to 1$, where the influence of noise is the most pronounced.

(ii) In the case of sufficiently large values of the carrying capacity, $K^* > K_c^*$, noise-induced relaxation oscillations are possible.

Figure 5 shows a phase diagram in the $\nu - a^2$ plane at $\alpha^* = 0.99$ and $K^* = 100$ ($K_c^* = 21.058$). The shaded region in the figure corresponds to those regions of the noise parameters, ν and a^2, where the oscillations of population sizes are possible. As the noise amplitude a decreases the region of oscillations narrows down and disappears at the critical value of the noise amplitude $a_c^2 = 0.7578$. Hence, there is an upper limit $a_c(\alpha^*, K^*)$ for the noise amplitude at lower values of which the system is characterized by just one stable equilibrium (limit cycles cannot occur). The boundary of the region of the oscillatory phase and the critical noise amplitude a_c are given by the system of transcendental equations:

$$\frac{d}{du}y(u) = 0, \qquad \frac{d^2}{du^2}y(u) = 0, \tag{34}$$

where $y(u)$ is given by equations (27) and (29). At a fixed K^* the critical parameter a_c increases monotonically to 1 if the prey capturing rate $\alpha^* \in (0,1)$ decreases. For $a \to 1$, from equations (34) we can easily obtain an asymptotical

expression for the boundaries of the region of oscillations $\nu_1(a^2)$ and $\nu_2(a^2)$:

$$\nu_i(a^2) \approx \frac{z_i[2(1-\alpha^*)+z_i(2-\alpha^*)]}{(1+z_i)|\ln(1-a^2)|}, \quad a \to 1, \qquad (35)$$

where $i = 1, 2$; z_1 and z_2 are the positive solutions of the transcendental equation

$$\left[1-\alpha^*+\frac{\alpha^* z}{2(1+z)}\right]^2 = 1-\alpha^*+\frac{\alpha^* e^z}{K^*(1+z)}, \quad K^* > K_c^*. \qquad (36)$$

It is remarkable that the region of the oscillations narrows down also in the vicinity of the maximal noise amplitude $a = 1$, and disappears at the point $\nu = 0$, $a = 1$. Thus, the phenomenon of noise-induced oscillations is absent in two cases: if the noise amplitude is either too low or very large. Furthermore, from Figure 5 it is seen that an increase of the noise correlation time, $\tau_c = 1/\nu$, can cause a transition from a stable equilibrium state to a state where both the predator-population and average prey-population densities oscillate. Notably, a further increase of τ_c causes a reentrant transition, i.e., the limit cycle disappears and the system approaches a stable equilibrium state. Therefore, in the fast-noise limit, $\tau_c \to 0$, and in the adiabatic limit, $\tau_c \to \infty$, oscillations are impossible. It is obvious that such transitions can also occur if the noise amplitude a is chosen as the control parameter. However, in this case, as a rule, a reentrant transition (for increasing a) from the oscillatory regime to an equilibrium state appears at a very large value of the noise amplitude $a \approx 1$, at which extinction due to demographic stochasticity is possible. Since the dynamics of the corresponding deterministic model (19) with the condition $\alpha^* < 1$ is characterized by a globally stable equilibrium, the asymptotic behavior described above has a distinct physical meaning. In the case of the adiabatic limit, $\tau_c \to \infty$, transitions between both states of the nonequilibrium noise $Z(t)$ are so rare that the system has enough time to allow deterministic dynamics to be formed between the transitions. At the fast-noise limit, $\tau_c \to 0$, i.e. at very high frequencies of colored fluctuations, the dynamics of the system is under the influence of the average $K_{eff}^{-1} := \langle K_i^{-1} \rangle = [K(1-a^2)]^{-1}$. Hence, the influence of fast fluctuations on an ecosystem can be biologically interpreted as a reduction of the carrying capacity K of single species in equation (12). Thus, our model with noise is, in the case of $\tau_c \to 0$, equivalent to a deterministic model with the carrying capacity K_{eff}. Let us note that such behavior of the system in the case of $\alpha^* < 1$ is more pronounced at a ratio-dependent limit, i.e., when predator interference is strong and is mainly the result of an interplay of predator interference and environmental fluctuations.

In Figure 6, noise-induced transitions different from those considered in Figure 5 can be observed on the phase diagram in the $u - \nu$ plane. Namely, in Figure 6 the lines $u_0(\nu)$, at different values of noise amplitudes, correspond to the equation

$$u_0(\nu) = K^*(1-a^2)\,{}_2F_1\left(\frac{1}{2}, 1; \frac{1}{2}+\frac{\nu}{2}; a^2\right), \qquad (37)$$

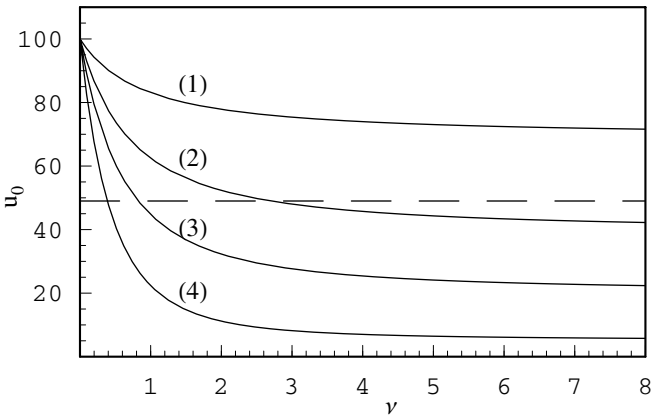

Fig. 6. Dependence of the critical parameter u_0 on the noise switching rate ν, obtained from equation (37) at different values of noise amplitudes a. Curves (1)–(4) correspond to the following values: $K^* = 100$; (1) $a^2 = 0.3$; (2) $a^2 = 0.6$; (3) $a^2 = 0.8$; (4) $a^2 = 0.95$. The dashed line corresponds to the predator isocline of equation (31) with $s = 0.98$. In the case of $u_0(\nu) < s/(1-s) = 49$ the predator population drives to extinction.

which determines noise-induced extinction of the predator population. The dashed horizontal line represents the predator isocline $u = s/(1-s)$ (see Eq. (31)). In the case of $s/(1-s) < u_0(\nu)$ both the prey and predator populations coexist either at a globally stable equilibrium or at a stable limit cycle. But if $u_0(\nu) < s/(1-s)$, the predators are unable to reproduce fast enough to compensate their death rate and consequently the predator population drives to extinction. So an increase of the switching rate ν of environmental fluctuations can cause extinction of the predator population. From Figure 6 it is seen that predator extinction occurs at lower values of the switching rate when the noise amplitude a increases. Note that, since in a ratio-dependent model the saturation constant $c = 0$, i.e. $K^* = \infty$, and thus such transitions are absent.

Next we will briefly consider the case of $\alpha^* > 1$. A major property of the proposed model at this regime is that an interplay of the colored-noise-induced quasibistability of the mean prey-population density and the Hopf bifurcating dynamics of the system (analogous to that in the deterministic case) can generate a rich variety of phase diagrams. Note first that, somewhat surprisingly, there exists a critical value of the prey capturing rate $\alpha_c^* \approx 1.1078$, above and below which the behavior of $\nu - a^2$ phase diagrams is qualitatively different.

In the case of $1 < \alpha^* < \alpha_c^*$, there are two positive solutions z_1^* and z_2^* of Eq. (33). According to equation (32) these solutions determine two critical carrying capacities: $K_{c1}^* < \alpha^*/(\alpha^*-1) < K_{c2}^*$. Hence, one can discern four cases. (i) If $K^* < K_{c1}^*$, then the system is monostable, i.e. no limit cycle can occur. (ii) For $K_{c1}^* < K^* < \alpha^*/(\alpha^*-1)$ the phase diagram on the $\nu - a^2$ plane is qualitatively similar to Figure 5. Thus, noise-induced transitions between the equilibrium state and the oscillating regime are possible. (iii) In the case of $\alpha^*/(\alpha^*-1) < K^* < K_{c2}^*$ a

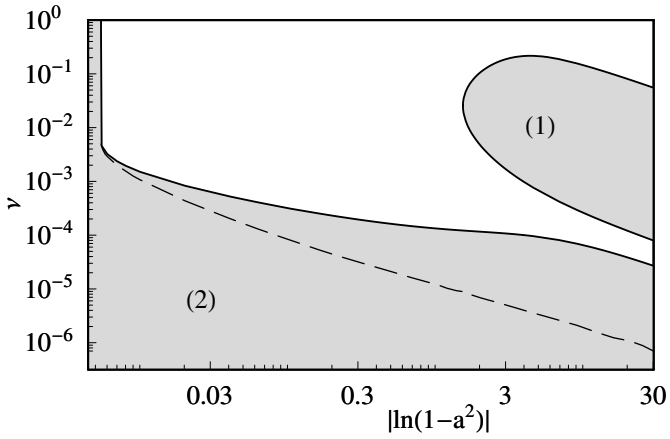

Fig. 7. (ν, a^2) phase diagram for the existence of limit cycles in the case of $\alpha^*/(\alpha^*-1) < K^* < K^*_{c2}$. The parameter values $\alpha^* = 1.05$ and $K^* = 21.115$ ($K^*_{c2} = 21.125$) are used. The shaded regions correspond to the two domains ((1) and (2)) where oscillations are possible. The borders of the domains are computed from equations (34), (27), (29), and (30). The dashed line depicts the lower border above which the relaxation oscillations are possible. For more details see the text.

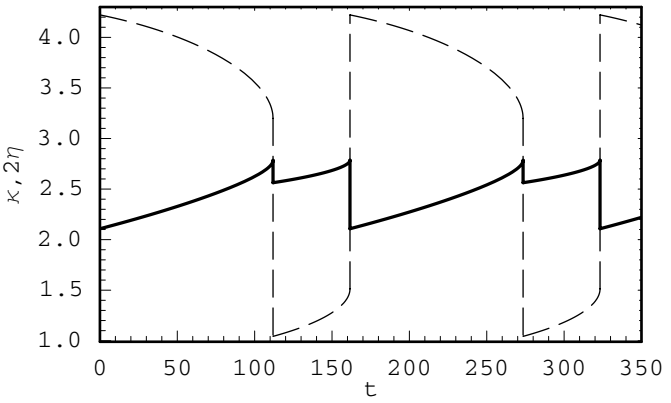

Fig. 8. The skewness κ and the coefficient of variation η of the distribution of the prey population sizes vs dimensionless time t, calculated by means of equations (26)–(30). Solid line: the function $\eta(t)$. Dashed line: the skewness function $\kappa(t)$. The parameter values are the same as in Figure 4.

typical phase diagram can be seen in Figure 7. The interesting peculiarity of the diagram is that there are two disconnected regions (the shaded areas in Fig. 7) where the limit cycles can appear. The upper domain (1) is qualitatively similar to the one represented in Figure 5 and corresponds to "purely" noise-induced relaxation oscillations. In the larger shaded region (2) the oscillations are related to noise-influenced "deterministic" limit cycles. Here we would like to remind the reader of the fact that the corresponding deterministic (the noise is absent) model (19) with conditions $\alpha^* > 1$ and $K^* > \alpha^*/(\alpha^*-1)$ can have a globally asymptotically stable limit cycle. It is also noteworthy that there is a critical value of the noise amplitude a_1 (not shown in Fig. 7, $a_1^2 = 0.00545$), namely

$$a_1^2 = 1 - \frac{\alpha^*}{K^*(\alpha^*-1)}, \tag{38}$$

below which oscillations (but not relaxation oscillations) can appear at all values of the noise correlation time. When $a > a_1$, the influence of the noise is thought to be a stabilizing factor, because an increase of the noise amplitude reduces rapidly the interval of the values of the switching rate ν where oscillations are possible. An important observation here is that relaxation oscillations occur only in the relatively small wedge-shaped area in domain (2) (the lower border of this region is indicated with the dashed line in Fig. 7). Other possible oscillations in domain (2) correspond to the prey isoclines of the form (2) and (3) in Figure 2 and will almost cause an extinction of the predator population or even the whole system (cf. the comments at the end of Section 3.1. (iv) For $K^* > K^*_{c2}$, the general view of the phase diagram is similar to Figure 7, but the "exclusion zone" between the domains (1) and (2) is absent.

In the case of $\alpha^* > \alpha^*_c \approx 1.108$ there are two possibilities. (i) If $K^* < \alpha^*/(\alpha^*-1)$, then the prey isocline $y(u)$ is a monotonically decreasing function of u for all values of the noise amplitude and correlation time, i.e. the system is always in an equilibrium state. (ii) When $K^* > \alpha^*/(\alpha^*-1)$, the phase diagram in the $\nu - a^2$ plane is qualitatively similar to the case of (iv) at $1 < \alpha^* < \alpha^*_c$.

Finally, we will briefly consider the behavior of the distribution of prey-subpopulation abundances during the relaxation cycle period. It is obvious that for a cyclic regime also the other statistical quantities characterizing the distribution of prey-subpopulations abundances, such as variance, skewness, and kurtosis, exhibit relaxation oscillations. The time series of the coefficient of variation η and skewness κ,

$$\eta = \frac{\sqrt{\langle (X - \langle X\rangle)^2\rangle}}{\langle X\rangle}, \qquad \kappa = \frac{\langle (X-\langle X\rangle)^3\rangle}{[\langle (X-\langle X\rangle)^2\rangle]^{3/2}}, \tag{39}$$

illustrate the fact, that η and κ are relatively large (see Fig. 8). In other words, subpopulation sizes are distributed widely and asymmetrically around the mean value. Let us note that, as a rule, at the region of the minima of the mean $\langle X\rangle$ the probability density $P(x,\rho)$ exhibits a bell-shaped form, whereas for the region of the maxima $P(x,\rho)$ exhibits a U-shaped form (see Eq. (24)). Therefore, in the latter case, there is a high probability that subpopulations with both high and low abundances are found, but the probability for moderate sizes is relatively small. Thus, the Gaussian distribution of species abundances, which is the most popular approximation generally used for the description of the dynamical properties of stochastic ecosystems [37] and some physical systems [38], is not applicable here.

4 Conclusions

We have generalized an $(N + 1)$-species predator–prey stochastic model [29] to the case of the Beddington functional response. The behavior of this model is analysed mainly in the region of the system parameters space, where the deterministic counterpart of the model is characterized by a globally asymptotically stable nontrivial equilibrium.

The influence of a fluctuating environment on the carrying capacities of prey subpopulations is modeled as a dichotomous noise. To obtain analytic results we study the model using a mean field approach in combination with the assumption that the growth rate of the predator is much smaller than the growth rates of the preys.

The presence of colored fluctuations of the carrying capacities of prey populations has a profound effect on the predator–prey system described by equations (18), rearranging its parameter space so that in certain regions colored noise can induce quasibistability of the mean prey-populations density. As a consequence there appear colored-noise-induced relaxation oscillations of the mean prey-abundance and predator-abundance, even in the case of $\alpha < b$, i.e., if the prey capturing rate α is lower than the predator interference intensity b. This result that the fluctuations of the carrying capacities of preys can induce a stable slow-fast limit cycle at $\alpha < b$ is somewhat surprising because, in the corresponding deterministic model (noise is absent), the appearance of limit cycles is impossible at any value of the carrying capacity K. The results indicate that the effect of noise is not merely restricted to the small shift of the critical capturing rate for Hopf bifurcations as in the particular case described in [29], but it will change the whole nature of the dynamics. Notably, transition from an equilibrium state to a limit cycle is possible only if the noise amplitude is greater than the critical value a_c (see Fig. 5). For sufficiently large noise amplitudes, $a > a_c$, an increase of the noise correlation time can cause oscillations of the mean prey-population and predator-population sizes. Moreover, the corresponding transitions are found to be reentrant, i.e. at a higher value of the correlation time oscillations disappear and the system approaches an equilibrium state.

We examined the phenomenon of colored-noise-induced oscillations in a particular case (ratio-dependent functional response) of model (18) already in [29]. However, in contrast to the present paper, our earlier study [29] considered only the case where the value of the noise amplitude was very small, and hence as a consequence, for the existence of noise-induced Hopf-bifurcations the prey capturing rate α must be located very near to the Hopf bifurcation point of the corresponding deterministic model, i.e. the parameter region of the deterministic counterpart where limit cycles are possible was considered. As was mentioned in Introduction, such oscillations are very sensitive to small variations of the system parameters and initial conditions, and therefore their importance in ecological context is doubtful.

Furthermore, noise-induced transitions different from those considered above can appear. For sufficiently large values of the saturation parameter c and the noise amplitude a the decrease of the noise correlation time causes extinction of the predator population (Fig. 6). Note that in the case of a ratio-dependent model such transitions are absent.

In conclusion, some, important from the ecological viewpoint, remarks must be made about the effects of the crucial parameters b and c on the existence of noise-induced slow-fast cycles. (i) For $b > \alpha$, the phenomenon of noise-induced relaxation oscillations is more pronounced at moderate values of interference, $b \approx \alpha$, and relatively small values of saturation $c < K/K_c^*$ (see Eq. (32)), e.g. in the case of ratio-dependence. Note that the phenomenon appears also at $b > \alpha$, however the critical noise amplitude a_c, below which there are no relaxation oscillations, increases rapidly as interference increases. (ii) In the case of sufficiently large values of saturation (prey-dependence dominates), the oscillatory regime is impossible and the dynamics of the system converges to an equilibrium. (iii) When both indicators, interference and saturation, are sufficiently low, $b < \alpha$ and $c < K(\alpha - b)/\alpha$, the conditions of validity of the relaxation dynamics are not fulfilled anymore and apart from relaxation cycles oscillations of another character appear. In the case of those oscillations the dynamics can approach very small values of the mean prey-abundance and extinction of the whole system may occur in nature due to demographic stochasticity, even if we have a stable cycle mathematically. Generally, environmental fluctuations prevent such oscillations (extinction), but the critical noise amplitude above which prevention is considerable, increases relatively rapidly as the saturation parameter decreases (cf. Fig. 7 and Eq. (38)).

Our main conclusion is that an interplay of mutual interference between predators and environmental fluctuations can be one of the possible mechanisms for the spontaneous generation of a slow-fast oscillatory regime through predator-prey trophic interaction in predator–prey communities. Under some conditions the model communities fluctuate in gradually changing regimes, which at times shift sharply to alternative regimes. Note that no dramatic extremes in the characteristic parameters of environmental fluctuations are needed to invoke such switches.

The phenomena are robust enough to survive a modification of the noise as well as the prey's self-regulation mechanism. The noise, for example, can be either a trichotomous noise [39] or a more complicated telegraph process, and logistic self-regulation can be replaced with a generalized Verhulst self-regulation mechanism (cf. [29]). Although the concrete formulas are different, the general picture of colored-noise-induced transitions is the same as that encountered in Section 3.

Finally, we believe that the results discussed here provide a possible alternative scenario for transitions from an equilibrium state to a limit cycle (and the opposite way) observed in nature.

This research was partly supported by the Estonian Science Foundation Grants No. 5943 and 7048, and the International Atomic Energy Agency Grant No. 12062.

References

1. L. Gammaitoni, P. Hänggi, P. Jung, F. Marchesoni, Rev. Mod. Phys. **70**, 223 (1998)
2. J. García-Ojalvo, J.M. Sancho, *Noise in Spatially Extended Systems* (Springer Verlag, New York, 1999)
3. P. Reimann, Phys. Rep. **361**, 57 (2002)
4. Hu Gang, T. Ditzinger, C.Z. Ning, H. Haken, Phys. Rev. Lett. **71**, 807 (1993); A.S. Pikovsky, J. Kurths, Phys. Rev. Lett. **78**, 775 (1997); A. Neiman, P.I. Saparin, L. Stone, Phys. Rev. E **56**, 270 (1997); B. Lindner, J. García-Ojalvo, A. Neiman, L. Schimansky-Geier, Phys. Rep. **392**, 321 (2004); C.B. Muratov, E. Vanden-Eijnden, E. Weinan, Physica D **210**, 227 (2005)
5. S.L. Ginzburg, M.A. Pustovoit, Phys. Rev. Lett. **80**, 4840 (1998); S.L. Ginzburg, M.A. Pustovoit, Phys. Lett. A **291**, 77 (2001); I. Bena, C. Van den Broeck, R. Kawai, K. Lindenberg, Phys. Rev. E **66**, 045603(R) (2002); R. Mankin, A. Haljas, R. Tammelo, D. Martila, Phys. Rev. E **68**, 011105 (2003); A. Rekker, R. Mankin, R. Tammelo, Physica E **29**, 419 (2005)
6. S. Kim, S.H. Park, C.S. Ryu, Phys. Rev. Lett. **78**, 1616 (1997); R. Müller, K. Lippert, A. Kühnel, U. Behn, Phys. Rev. E **56**, 2658 (1997); A.A. Zaikin, J. García-Ojalvo, L. Schimansky-Geier, Phys. Rev. E **60**, R6275 (1999); Yu.V. Gudyma, Physica A **331**, 61 (2004)
7. A. Sauga, R. Mankin, Phys. Rev. E **71**, 062103 (2005)
8. S. Leibler, Nature **370**, 412 (1994); O.M. Braun, Yu.S. Kivshar, Phys. Rep. **306**, 1 (1998); P.S. Landa, P.V.E. McClintock, Phys. Rep. **323**, 1 (2000); F. Jülicher, A. Ajdari, J. Prost, Rev. Mod. Phys. **69**, 1269 (1997)
9. Special issue, edited by E. Linke (guest editor), Appl. Phys. A **75**, No. 2, 167 (2002); A. Pankratov, B. Spagnolo, Phys. Rev. Lett. **93**, 177001 (2004)
10. J.M.G. Vilar, R.V. Solé, Phys. Rev. Lett. **80**, 4099 (1998); G. Abramson, D.H. Zanette, Phys. Rev. E **57**, 4572 (1998); B. Houchmandzadeh, Phys. Rev. E **66**, 052902 (2002); B. Drossel, A. McKane, J. Theor. Biol. **204**, 467 (2000); P. Chesson, Theor. Popul. Biol. **64**, 345 (2003); N. Kinezaki, K. Kawazaki, F. Takasu, N. Shigesada, Theor. Popul. Biol. **64**, 291 (2003); V. Kaitala, E. Ranta, Proc. R. Soc. Lond. B **268**, 1769 (2001); A. McKane, D. Alonso, R.V. Solé, Phys. Rev. E **62**, 8466 (2000); A. Caruso, M.E. Gargano, D. Valenti, A. Fiasconaro, B. Spagnolo, Fluct. Noise Lett. **5**, L349 (2005); A. Fiasconaro, D. Valenti, B. Spagnolo, Eur. Phys. J. B **50**, 189 (2006); D. Valenti, L. Schimansky-Geier, X. Sailer, B. Spagnolo, Eur. Phys. J. B **50**, 199 (2006); F.C. Poderoso, J.F. Fontanari, Phys. Rev. E **74**, 051919 (2006)
11. B. Spagnolo, M. Cirone, A. La Barbera, F. de Pasquale, J. Phys.: Condens. Matter **14**, 2247 (2002)
12. D. Valenti, A. Fiasconaro, B. Spagnolo, Physica A **331**, 477 (2004)
13. A. Fiasconaro, B. Spagnolo, Acta Phys. Pol. B **38**, 1775 (2007)
14. B. Spagnolo, D. Valenti, A. Fiasconaro, Math. Biosci. Engineer. **1**, 185 (2004); D. Valenti, L. Schimansky-Geier, X. Sailer, B. Spagnolo, M. Iacomi, Acta Phys. Pol. B **38**, 1961 (2007)
15. P. Turchin, *Complex Population Dynamics: A Theoretical/Empirical Synthesis* (Princeton University Press, Princeton, 2003)
16. *Population Cycles: The Case for Trophic Interactions*, edited by A.A. Berryman (Oxford University Press, Oxford 2002)
17. L. Becks, F.M. Hilker, H. Malchov, K. Jürgens, H. Arndt, Nature **435**, 1226 (2005); W.A. Nelson, E. McCauley, F.J. Wrona, Nature **433**, 413 (2005); T. Yoshida, L.E. Jones, S.P. Ellner, G.F. Fussmann, N.G. Hairston Jr, Nature **424**, 303 (2003); G.F. Fussmann, S.P. Ellner, K.W. Shertzer, N.G. Hairston Jr, Science **290**, 1358 (2000)
18. R. Arditi, L.R. Ginzburg, J. Theor. Biol. **139**, 311 (1989)
19. P.A. Abrams, Ecology **75**, 1842 (1994); H.R. Akçakaya, R. Arditi, L.R. Ginzburg, Ecology **76**, 995 (1995)
20. D. Alonso, F. Bartumeus, J. Catalan, Ecology **83**, 28 (2002)
21. C. Jost, O. Arino, R. Arditi, Bull. Math. Biol. **61**, 19 (1999); D. Xiao, S. Ruan, J. Math. Biol. **43**, 268 (2001); F. Berezovskaya, G. Karev, R. Arditi, J. Math. Biol. **43**, 221 (2001); Y. Kuang, E. Beretta, J. Math. Biol. **36**, 389 (1998); S.–B. Hsu, T.–W. Hwang, Y. Kuang, J. Math. Biol. **42**, 489 (2001)
22. L.S. Luckinbill, Ecology **54**, 1320 (1973); R. Arditi, A.A. Berryman, TREE **6**, 32 (1991); R. Arditi, L.R. Ginzburg, H.R. Akcakaya, Am. Nat. **138**, 1287 (1991); R. Arditi, N. Perrin, H. Saiah, OIKOS **60**, 69 (1991); I. Hanski, TREE **6**, 141 (1991); H.R. Akcakaya, R. Arditi, L.R. Ginzburg, Ecology **76**, 995 (1995); C. Cosner, D.L. DeAngelis, J.S. Ault, D.B. Olson, Theor. Popul. Biol. **56**, 65 (1999)
23. P.A. Abrams, L.R. Ginzburg, TREE **15**, 337 (2000)
24. R. Arditi, J.–M. Callois, Y. Tyutyunov, C. Jost, C.R. Biologies **327**, 1037 (2004)
25. J.R. Beddington, J. Anim. Ecol. **45**, 331 (1975)
26. D.L. DeAngelis, R.A. Goldstein, R.V. O'Neill, Ecology **56**, 881 (1975)
27. G. Huisman, R.J. de Boer, J. Theor. Biol. **185**, 389 (1997)
28. R.S. Cantrell, C. Cosner, J. Math. Anal. Appl. **257**, 206 (2001); T.W. Hwang, J. Math. Anal. Appl. **290**, 113 (2004)
29. R. Mankin, T. Laas, A. Sauga, A. Ainsaar, E. Reiter, Phys. Rev. E **74**, 021101 (2006)
30. M. Bandyopadhyay, J. Chattopadhyay, Nonlinearity **18**, 913 (2005)
31. W. Horsthemke, R. Lefever, *Noise-induced Transitions* (Springer–Verlag, Berlin, Heidelberg, New York, Tokyo, 1984)
32. *Advanced Ecological Theory: Principles and Applications*, edited by J.M. McGlade (Blackwell Science, Oxford, 1999)
33. R. Mankin, A. Sauga, A. Ainsaar, A. Haljas, K. Paunel, Phys. Rev. E **69**, 061106 (2004)
34. S. Rinaldi, M. Scheffer, Ecosystems **3**, 507 (2000)
35. M. Scheffer, S. Carpenter, J.A. Foley, C. Folke, B. Walker, Nature **413**, 591 (2001); J. Vandermeer, P. Yodzis, Ecology **80**, 1817 (1999); E.H. van Nes, M. Scheffer, Am. Nat. **164**, 255 (2004)
36. D. Ludwig, D.D. Jones, C.S. Holling, J. Animal. Ecol. **47**, 315 (1978)
37. H. Rieger, J. Phys. A **22**, 3447 (1989); R. May, Nature **238**, 413 (1972)
38. R. Kawai, X. Sailer, L. Schimansky–Geier, C. Van den Broeck, Phys. Rev. E **69**, 051104 (2004)
39. R. Mankin, A. Ainsaar, A. Haljas, E. Reiter, Phys. Rev. E **65**, 051108 (2002); R. Mankin, A. Ainsaar, E. Reiter, Phys. Rev. E **60**, 1374 (1999)